

The role of quantum-confined excitons vs defects in the visible luminescence of SiO₂ films containing Ge nanocrystals

K. S. Min,^{a)} K. V. Shcheglov, C. M. Yang, and Harry A. Atwater
Thomas J. Watson Laboratory of Applied Physics, California Institute of Technology, Pasadena, California 91125

M. L. Brongersma and A. Polman
FOM Institute for Atomic and Molecular Physics, Kruislaan 407, 1098 SJ Amsterdam, The Netherlands

(Received 10 October 1995; accepted for publication 22 February 1996)

Synthesis of Ge nanocrystals in SiO₂ films is carried out by precipitation from a supersaturated solid solution of Ge in SiO₂ made by Ge ion implantation. The films exhibit strong room-temperature visible photoluminescence. The measured photoluminescence peak energy and lifetimes show poor correlations with nanocrystal size compared to calculations involving radiative recombination of quantum-confined excitons in Ge quantum dots. In addition, the photoluminescence spectra and lifetime measurements show only a weak temperature dependence. These observations strongly suggest that the observed visible luminescence in our samples is not due to the radiative recombination of quantum-confined excitons in Ge nanocrystals. Instead, observations of similar luminescence in Xe⁺-implanted samples and reversible PL quenching by hydrogen or deuterium suggest that radiative defect centers in the SiO₂ matrix are responsible for the observed luminescence. © 1996 American Institute of Physics. [S0003-6951(96)02618-6]

Recently, a considerable amount of research has been devoted to the luminescence of group IV semiconductors of low dimensionality to study quantum-confined electronic states and to develop integrated optoelectronic devices directly on Si. Much of this effort was inspired by the discovery of visible room-temperature photoluminescence (PL) in porous silicon,¹ synthesized by anodic etching of Si. Since then, many other methods for synthesizing luminescent group IV nanocrystals have been reported. Nanocrystals embedded in a SiO₂ matrix offer an attractive option because SiO₂ is a well-characterized material known to passivate semiconductor surfaces. For Ge, most reports of visible PL from low-dimensional structures have involved Ge nanocrystals embedded in SiO₂.²⁻⁶

Three principle methods have been employed to synthesize Ge nanocrystals in SiO₂: rf cosputtering of Ge and SiO₂,²⁻⁴ hydrothermal reduction of Si_xGe_{1-x}O₂,⁵ and Ge ion implantation.⁶ For all methods of synthesis, similar visible PL spectra have been observed. Despite many suggestions, the origin of visible PL has not yet been made clear. The principal debate regarding the origin of luminescence seems to be whether or not the luminescence mechanism can be attributed to the radiative recombination of quantum-confined electron/hole pairs (or excitons) in Ge quantum dots.²⁻⁶ In this letter, we report results of experiments on Ge nanocrystals in SiO₂ made by ion implantation which indicate that the dominant process responsible for visible PL observed from SiO₂ containing Ge nanocrystals is *not* the radiative recombination of quantum-confined excitons in Ge nanocrystals. Instead, evidence from PL peak energy and lifetime measurements as a function of nanocrystal size, temperature dependent PL measurements, studies on luminescence from Xe⁺-implanted thermal SiO₂, and studies on the effect of hydrogen and deuterium on PL all strongly suggest

that the visible PL is primarily due to luminescent defect centers in the matrix.

SiO₂ films, 100 nm thick, grown by wet thermal oxidation on lightly *p*-doped (100) Si wafers were implanted at room temperature with 70 keV ⁷⁴Ge⁺ at doses of 1 × 10¹⁶/cm², 2 × 10¹⁶/cm², and 5 × 10¹⁶/cm². The energy was chosen such that the implanted Ge concentration profile is completely within the oxide film, with the peak concentration lying 30–40 nm from the surface. For the three implantation doses, the peak concentrations are 3, 6, and 13 at. % Ge, respectively, as determined by Rutherford backscattering spectrometry. After implantation, the samples were annealed in high vacuum at 600, 800, and 1000 °C for 40 min. We have previously performed extensive transmission electron microscopy (TEM) characterization on these samples and the average nanocrystal sizes were determined from Gaussian fits to the size distributions.⁷ For the 6 at. % Ge samples, the average sizes are 1.9, 3.2, and 7.2 nm, with full widths at half-maximum of 1.5, 3.4, and 4.0 nm, for the samples annealed at the three temperatures, respectively. It was also discovered that higher implantation doses yield samples with higher nanocrystal density, but with similar average sizes and size distributions after annealing.

Photoluminescence spectra were taken with 100 mW/mm² excitation using 457.9 nm Ar laser radiation, detected with an InGaAs photomultiplier and a grating spectrometer with a spectral resolution of 3.2 nm. The sample temperature was controlled between 12 and 300 K by a closed-cycle He cryostat. All spectra have been corrected for the photomultiplier and grating efficiencies. A very weak PL was observed from annealed as-grown SiO₂ films. Figure 1(a) shows the room-temperature PL spectra of the 6 at. % Ge sample, as-implanted and annealed at different temperatures. Several notable characteristics of the PL spectra in Fig. 1(a) have also been reported previously for SiO₂ containing Ge nanocrystals synthesized by other methods.²⁻⁶ First, only

^{a)}Electronic mail: ksmin@daedalus.caltech.edu

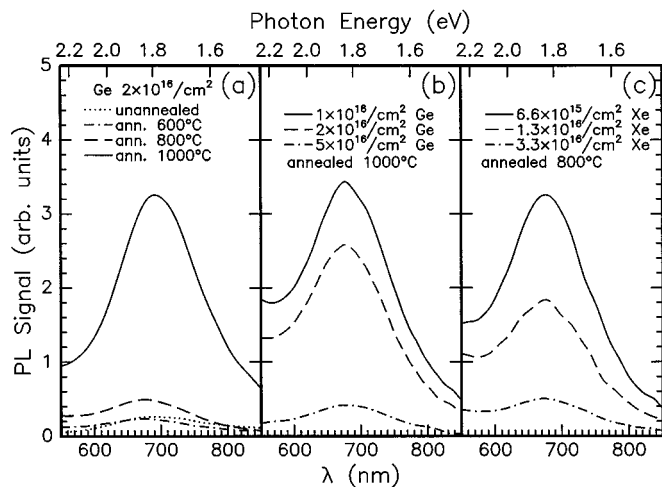


FIG. 1. Room-temperature visible PL spectra of 70 keV Ge^+ -implanted and 120 keV Xe^+ -implanted 100 nm thick SiO_2 on Si. (a) $2 \times 10^{16}/\text{cm}^2$ Ge^+ -implanted films, as-implanted and annealed at 600, 800, and 1000 $^\circ\text{C}$. (b) Ge^+ -implanted films with doses of $1 \times 10^{16}/\text{cm}^2$, $2 \times 10^{16}/\text{cm}^2$, and $5 \times 10^{16}/\text{cm}^2$, annealed at 1000 $^\circ\text{C}$ for 40 min; (c) Xe^+ -implanted films with doses of $6.6 \times 10^{15}/\text{cm}^2$, $1.3 \times 10^{16}/\text{cm}^2$, and $3.3 \times 10^{16}/\text{cm}^2$, annealed at 800 $^\circ\text{C}$ for 40 min.

a weak PL signal is observed for the unannealed sample compared to the annealed samples. Second, the annealed samples show an intense PL signal, visible to the unaided eye, with characteristically broad spectra. Third, no appreciable shift in peak luminescence energy is observed with variation in the annealing temperature (i.e., nanocrystal size). Figure 2 shows a plot of the peak luminescence energy of the measured PL spectra as a function of nanocrystal diameter for the same set of samples as in Fig. 1(a). The horizontal and vertical error bars indicate the FWHM of the nanocrystal size distributions and PL spectra, respectively. For comparison, a calculated variation of exciton transition energy as a function of the quantum dot diameter is also shown.⁸ High

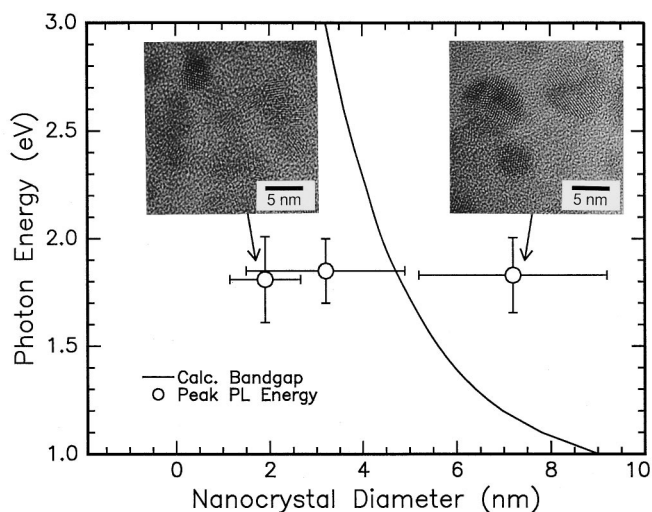


FIG. 2. A comparison between measured peak PL energy [from Fig. 1(a)] and calculated exciton energy (from Ref. 8) as a function of nanocrystal diameter. Horizontal and vertical error bars indicate the FWHM of the nanocrystal size distributions and PL spectra, respectively. High resolution TEM images of Ge nanocrystals corresponding to the highest and the lowest annealing temperatures are shown as insets.

resolution TEM images of the samples with the smallest and the largest nanocrystals are shown as insets in Fig. 2. For the nanocrystal size range in our samples (1.9–7.2 nm), the calculation predicts a variation of exciton energy from over 3 eV to less than 1.5 eV. Our experimental data in Fig. 2, however, exhibit no appreciable shift in peak luminescence energy, similar to other reports on SiO_2 , containing Ge nanocrystals.^{2–6} To our knowledge, no experimental observation of large PL peak energy shifts, comparable to those predicted by calculations, has been reported for Ge nanocrystals. The reported values⁴ of PL peak energy shift are an order of magnitude smaller than what has been predicted⁸ for radiative recombination of quantum-confined excitons.

Ion implantation creates a defect density in the SiO_2 network that far exceeds the equilibrium value. As it is already known that some defects in SiO_2 and $\text{Ge}_x\text{Si}_{1-x}\text{O}_2$ exhibit visible luminescence,⁹ it is very important to characterize the luminescence due to these irradiation-induced defects. To address this issue, we have performed 120 keV $^{130}\text{Xe}^+$ implantation into 100 nm SiO_2 films on Si at doses of $6.6 \times 10^{15}/\text{cm}^2$, $1.3 \times 10^{16}/\text{cm}^2$, and $3.3 \times 10^{16}/\text{cm}^2$. The energy and the three doses were carefully chosen using the TRIM Monte Carlo code,¹⁰ such that the projected range, the straggle, and the peak concentration of atomic displacements would closely resemble the atomic displacement profiles created by the three different Ge^+ implantation doses. We compare room-temperature PL spectra of Ge^+ -implanted samples and Xe^+ -implanted samples in Figs. 1(b) and 1(c). Figure 1(b) shows the room-temperature PL spectra of the Ge^+ -implanted samples annealed at 1000 $^\circ\text{C}$ for 40 min for the three Ge^+ doses. Figure 1(c) shows the room-temperature PL spectra of the Xe^+ -implanted samples annealed at 800 $^\circ\text{C}$ for 40 min for the three Xe^+ doses. The similarities in spectral features between Ge^+ -implanted samples and Xe^+ -implanted samples are strikingly clear. Strong visible room-temperature PL was observed in both samples only after annealing. The PL intensity decreases with increasing implantation dose for the annealed samples. It was also observed that the PL peak energy at ~ 680 nm (1.83 eV) and the spectrum shape does not depend on the annealing temperature. As one would not expect visible PL from the implanted Xe atoms themselves, these similarities in the PL spectra are very likely a result of the similarities in defect profiles created by ion irradiation in both the Ge^+ -implanted and Xe^+ -implanted samples.

Hydrogen is known to passivate electronic defects in semiconductors. Even the performance of an oxide-passivated Si p - n diode can be further improved upon hydrogenation, because oxygen, being a large atom, cannot passivate every dangling bond at the oxide/semiconductor interface.¹¹ By analogy, if there are dangling bonds at the nanocrystal/matrix interface that act as nonradiative recombination centers for quantum-confined electron-hole pairs (or excitons) in nanocrystals, hydrogen passivation would lead to an enhancement of the luminescence efficiency, hence higher PL intensity. We have thus performed passivation experiments using deuterium. Deuterium was used instead of hydrogen in order to facilitate concentration determination. Deuterium implantation was performed on annealed Ge^+ -implanted samples using a Kauffman ion beam source

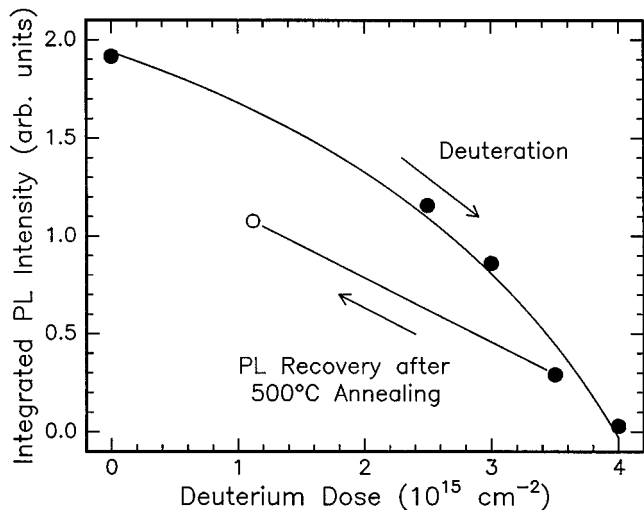


FIG. 3. Integrated PL intensity as a function of implanted deuterium dose for 6 at. % Ge sample annealed at 1000 °C for 40 min (closed circles). The open circle indicates the D concentration and the recovered PL intensity, after deuterium outdiffusion, of the sample with an original D dose of $3.5 \times 10^{15}/\text{cm}^2$. Solid lines are guides to the eye.

at a beam energy of 600 eV. An estimate of the projected range of 600 eV D^+ in SiO_2 using the TRIM code¹⁰ yields a value of about 25 nm. Although this range does not coincide with the projected ranges of Ge^+ implantations, previously reported values on the diffusivities of hydrogen atoms and molecules suggest that H and D will easily diffuse through an oxide film of 100 nm in laboratory time frame at room temperature.¹² Figure 3 shows the integrated PL intensity variation with deuterium concentration for the 6 at. % Ge sample, annealed at 1000 °C for 40 min. The implanted D doses range from $2 \times 10^{15}/\text{cm}^2$ to $4 \times 10^{15}/\text{cm}^2$, as determined by elastic recoil spectrometry using a 2 MeV $^4\text{He}^{++}$ beam. The introduction of atomic D drastically reduces the luminescence intensity, with nearly zero intensity for a D dose of $4.0 \times 10^{15}/\text{cm}^2$. Deuterium can be removed from the SiO_2 film by thermal annealing in vacuum. Elastic recoil spectrometry measurements indicate that $\sim 70\%$ of the original D concentration has diffused out of the film after a 30 min anneal at 500 °C. As shown in Fig. 3, up to $\sim 60\%$ of the original intensity is recovered after such an anneal. The spectral features remain unchanged.

To verify that these observations are due to the chemical effect of D rather than a physical effect such as D irradiation damage, we have also performed rapid thermal annealing on the 1000 °C-annealed 6 at. % Ge sample in dilute forming gas (3:97 $\text{H}_2:\text{N}_2$) at 800 °C under atmospheric pressure. As in the D^+ -implanted samples, a significant reduction in PL intensity was observed. A recovery of PL intensity upon out-diffusion of hydrogen was also observed.

Temperature dependent PL measurements provide further evidence against the applicability of the quantum-confined exciton model to our results. Temperature dependent PL measurements were performed on 6 at. % Ge samples annealed at two different temperatures, 600 and 1000 °C, corresponding to nanocrystal diameters of 1.9 and 7.2 nm. Very similar temperature dependencies of PL intensity were observed for the two samples. Both samples

showed only weak intensity variations with measurement temperature, varying only by a factor of 2 in the temperature range of 12–300 K. Spectral shapes showed no variation with temperature. No meaningful information could be deduced from a plot of log intensity as a function of inverse temperature. According to calculations,⁸ the exciton binding energy is expected to increase from ~ 50 meV to over 150 meV as the nanocrystal diameter decreases from 7.2 to 1.9 nm. One expects, therefore, a significant difference in the temperature dependence of PL spectra for different nanocrystal diameters, which we do not observe.

Finally, PL lifetime measurements were performed at various energies in the PL spectra and at various temperatures in the range of 12–300 K for all samples using a photomultiplier tube in a multichannel photon counting arrangement. The time resolution of our experimental setup was 100 ns. The calculated radiative lifetime⁸ ranges from ns to ms for Ge quantum dot diameters ranging from 1 to 3 nm. However, for our samples ranging from 1.9 to 7.2 nm in diameter, all measured PL lifetimes were at or below the experimental resolution, thus putting an upper bound of the lifetime at 100 ns. A relatively weak dependence of PL lifetimes on the nanocrystal size further supports the idea that the observed PL in our samples is not related to the radiative recombination of quantum-confined excitons in Ge nanocrystals.

These results have many implications, in light of many recent developments in the synthesis of nanocrystalline semiconductors in SiO_2 matrices by ion beam techniques as well as other methods. This is especially true since defects in SiO_2 are created not just during ion implantation processes, but are intrinsic to most synthesis techniques.

The authors acknowledge F. W. Saris, G. N. van den Hoven, and R. P. Camata for fruitful discussions, and M. Easterbrook, J. Derks, and J. ter Beek for technical assistance. This work was supported by the U. S. Department of Energy, Basic Energy Sciences, and NATO Ministry for Scientific Affairs. The work at FOM was financially supported by NWO, STW, and IOP Electro-Optics.

¹L. T. Canham, Appl. Phys. Lett. **57**, 1046 (1990).

²Y. Maeda, N. Tsukamoto, Y. Yazawa, Y. Kanemitsu, and Y. Matsumoto, Appl. Phys. Lett. **59**, 3168 (1991).

³Y. Kanemitsu, H. Uto, Y. Matsumoto, and Y. Maeda, Appl. Phys. Lett. **61**, 2187 (1992).

⁴Y. Maeda, Phys. Rev. B **51**, 1658 (1994).

⁵D. C. Paine, C. Caragianis, T. Y. Kim, Y. Shigesato, and T. Ishahara, Appl. Phys. Lett. **62**, 2842 (1993).

⁶H. A. Atwater, K. V. Shcheglov, S. S. Wong, K. J. Vahala, R. C. Flagan, M. L. Brongersma, and A. Polman, Mater. Res. Soc. Symp. Proc. **316**, 409 (1994).

⁷C. M. Yang, K. V. Shcheglov, M. L. Brongersma, A. Polman, and H. A. Atwater, Mater. Res. Soc. Symp. Proc. **358**, 181 (1995).

⁸T. Takagahara and K. Takeda, Phys. Rev. B **46**, 15578 (1992).

⁹K. Awazu, K. Muta, and H. Kawazoe, J. Appl. Phys. **74**, 2237 (1993); L. Skuja, J. Non-Cryst. Solids **179**, 51 (1994).

¹⁰J. F. Ziegler, J. P. Biersack, and U. Littmark, *The Stopping and Range of Ions in Solids* (Pergamon, New York, 1985).

¹¹J. I. Pankove and M. L. Tarng, Appl. Phys. Lett. **34**, 156 (1979).

¹²D. L. Griscom, J. Appl. Phys. **58**, 2524 (1985).